Thyroid hormones act as a timer for the postnatal maturation of parvalbumin neurons in the neocortex

Juan Ren[1,3], Suzy Markossian[1], Romain Guyot[1], Denise Aubert[1], Jacques Brocard[2], Jiemin Wong[3], Frédéric Flamant[1,*], Sabine Richard[1]

[1] Ecole Normale Supérieure de Lyon, INRAE, CNRS, Institut de Génomique Fonctionnelle de Lyon, 69364 Lyon, France

[2] Université Claude Bernard Lyon 1, CNRS UAR3444, Inserm US8, ENS de Lyon, SFR Biosciences, Lyon 69007, France

[3] Shanghai Key Laboratory of Regulatory Biology, Institute of Biomedical Sciences and School of Life Sciences, East China Normal University, 200241, Shanghai, China

[*] Corresponding author. Frederic.flamant@ens-lyon.fr Tel: 00 (33) 4 26 73 13 32

Abbreviated title: Thyroid hormone action in postnatal cortex

Declaration of conflict of interest: none.

Abstract

Thyroid hormones (THs) are required for proper maturation of parvalbumin-expressing GABAergic interneurons in the mouse neocortex, which function is essential to maintain a proper balance between neuronal excitation and inhibition. However, the timeline of this TH action has yet to be elucidated. Here, we used several mouse models expressing dominant negative mutations of the TH nuclear receptor α1 (TRα1), to better define the time window during which THs promote the maturation of parvalbumin neurons. The action of THs during the first three postnatal weeks appears to be necessary to initiate the elaboration of a specialized extracellular matrix called the perineuronal net. Transcriptome analysis identified a small set of putative target genes for TRα1, which are at the origin of the postnatal remodeling of the repertoire of ions channels and the elaboration of perineuronal nets. These data suggest that THs act as a timer to define the temporal boundaries of the critical period of heightened cortical plasticity, which plays a fundamental role in the development of neuronal circuits.

Significance statement

Thyroid hormones exert a major influence on late neurodevelopment, acting directly on gene expression by binding to nuclear receptors present in all cell types. This study reports the discovery of a direct link between the transcriptional regulation exerted by the thyroid hormones in GABAergic neurons and the timing of the critical period of heightened plasticity. This provides a general framework to understand the pathology associated with altered thyroid hormone signaling.

Keywords

Thyroid hormones / TRα1 / PV neurons / GABAergic neurons / neocortex

Introduction

Parvalbumin-expressing neurons (PV neurons) are GABAergic inhibitory interneurons that play a central role in the organization of neuronal circuits in the neocortex (Hijazi, Smit et al., 2023). They are fast-spiking and synchronize network oscillations, which are thought to play an important role in information processing and memory formation. In mice, PV neurons begin to express parvalbumin during the first postnatal weeks (del Rio, de Lecea et al., 1994, Huang, Kirkwood et al., 1999). During this time, the electrical activity of these neurons progressively increases (Okaty, Miller et al., 2009) and synaptogenesis is very active. This opens the so-called critical period of heightened synaptic plasticity (Hensch, 2005) during which sensory input and experience shape neuronal networks in the neocortex. The critical period ends when circuit rewiring becomes actively dampened (Takesian & Hensch, 2013). Notably, the elaboration of the perineuronal net (PNN) around PV neurons, a densely packed extracellular matrix enriched in proteoglycans, stabilizes synapses and restricts plasticity (Wingert & Sorg, 2021). Defects in PV neuron maturation during the critical period cause a persistent imbalance between neuronal excitation and inhibition, which is suspected to be at the origin of several pathological conditions, including attention deficit hyperactivity disorder, autism, and epilepsy (Sohal & Rubenstein, 2019).

THs (including T3 or 3,3',5-triiodo-L-thyronine, and the less active precursor T4 or thyroxine) exert a broad influence on brain development, and they are critically required for proper maturation of PV neurons (Bernal, Morte et al., 2022, Ren & Flamant, 2023, Richard, Ren et al., 2023). THs directly act on gene transcription by binding to the TRα1 and TRβ1/2 nuclear receptors, which are encoded by the *Thra* and *Thrb* genes in mice. In both humans and mice, TRα1 mutations have dramatic and irreversible consequences on neurodevelopment, and these consequences are similar to those of TH

59 deficiency, with most human presenting with mild to severe intellectual disability (Berbel, Navarro et
60 al., 2014, van Gucht, Moran et al., 2017).

61 In the postnatal mouse neocortex, PV neurons display a high sensitivity to TRα1 mutation (Wallis,
62 Sjogren et al., 2008) and TH deficiency (Mayerl & Heuer, 2023, Uchida, Hasuoka et al., 2021). We
63 have previously found that expressing TRα1^{L400R}, a dominant-negative TRα1 receptor, only in the
64 GABAergic lineage from an early neurodevelopmental stage, was sufficient to dramatically inhibit the
65 expression of parvalbumin and the elaboration of PNNs (Richard, Guyot et al., 2020). By contrast, we
66 have recently observed that expressing TRα1^{L400R} specifically in PV neurons had no visible effects on
67 their maturation and had only moderate consequences on their function (Okaty et al., 2009). In the
68 latter study, the specific blockade of TH signaling in PV neurons was driven by the expression of the
69 *Pvalb* gene, which starts very gradually and with considerable temporal variation between PV
70 neurons, ranging from a few days up to several weeks after birth (de Lecea, del Rio et al., 1995).
71 Taken together, these results suggest that TH signaling stimulates the maturation of PV neurons
72 during a specific time window and then becomes less important to maintain their function.
73 Accordingly, the appearance of hypothyroidism in adult stages does not prevent the expression of
74 parvalbumin (Gilbert, Sui et al., 2007, Uchida et al., 2021). However, the boundaries of the time
75 window during which THs act on PV neuron maturation remain elusive. Moreover, whether blocking
76 TH signaling during development only delays or permanently inhibits PV neuron maturation remains
77 an open question.

78 To gain more insight into the timeline of TH action on PV neuron maturation, we generated novel
79 mouse models to restrict the expression of dominant-negative TRα1 receptors in GABAergic neurons
80 during specific time windows. Histological observations of parvalbumin and PNNs in the
81 somatosensory cortex allowed us to pinpoint a key time window for TH action in PV neurons, around
82 the second postnatal week. Moreover, we evidenced a lifelong persistence of defects in PV neuron
83 maturation when TH signaling was blocked in GABAergic neurons from early stages of development.
84 A genome-wide analysis of GABAergic neuron transcriptome in the whole neocortex two weeks after
85 birth also allowed us to identify a set of genes whose regulation is expected to be involved in TH-
86 mediated maturation of PV neurons. Several of these genes are notably known to be linked to the
87 closure of the critical period. As a whole, our results show that THs, via their action on PV neurons,
88 play a key role in cortical circuit maturation in the mouse brain.

89 ***Results***

90 ***TRα1^{E395fs401X} expression in GABAergic neurons from an early developmental stage permanently***
91 ***inhibits PV neuron maturation***

92 In our previous work, we used Cre/loxP recombination to restrict the expression of the dominant-
93 negative TRα1^{L400R} mutant receptor in the GABAergic lineage from embryonic day 12.5 (Richard et al.,
94 2020). As most of the mice had frequent epileptic seizures and died before postnatal day 21 (PND21),
95 we could not address a possible recovery of PV neuron maturation during adulthood. We thus used
96 here a similar model, based on the *Thra^{Slox}* allele, encoding TRα1^{E395fs401X}, a receptor with moderate
97 dominant-negative activity (Markossian, Guyot et al., 2018). The floxed *ROSA-tdTomato^{lox}* reporter
98 transgene was also introduced to trace the cells belonging to the GABAergic lineage. One third of
99 *Thra$^{Slox/+}$ ROSA-tdTomato$^{lox/+}$ Gad2-Cre* mice survived to adulthood. We therefore compared these
100 mutant mice and *Thra$^{+/+}$ ROSA-tdTomato$^{lox/+}$ Gad2-Cre* littermates (controls), to histologically study
101 whether TRα1 mutation only delays or permanently inhibits PV neuron maturation.

102 At PND21, while the red fluorescence did not indicate any cell loss in the GABAergic lineage (Suppl.
103 Fig. 1), the density of parvalbumin-positive (PV+) cells was drastically lower in mutants than in
104 controls (Fig. 1a, b). PNNs were labeled using Wisteria Floribunda Agglutinin (WFA), which binds N-
105 acetyl-galactosamine-β1 residues of PNN glycoproteins. The density of WFA-positive (WFA+) cells
106 was also significantly lower in mutants (Fig. 1a, c). Interestingly, the two phenotypes were
107 accompanied by a clearly lower ratio of PV+ cells that were surrounded by PNNs in mutants,
108 compared to controls (Fig. 1a, d). At adult stage, the same analysis showed signs of some recovery of
109 PV neuron density in mutants (Fig. 1e, f), while the PNN defect persisted (Fig. 1e, g and h). Overall,
110 TRα1^{E395fs401X} appears to have a similar negative influence to TRα1^{L400R} and permanently impairs the
111 maturation of PV neurons.

112 ***Postnatal expression of TRα1^{L400R} in GABAergic neurons is sufficient to inhibit PV neuron***
113 ***maturation***

114 We have recently observed that the postnatal expression of TRα1^{L400R} in PV neurons has little effect
115 on their maturation (submitted data). Although adult *Thra$^{AMI/+}$ ROSA-tdTomato$^{lox/+}$ Pvalb-Cre* mice
116 displayed minor histological, electrophysiological and behavioral defects, they did not spontaneously
117 present epileptic seizures or lethality (Ren, Markossian et al., 2024). This suggests that TH signaling
118 intensively stimulates the maturation of PV neurons during a specific time window, and then
119 becomes secondary to maintain their function. To better evaluate the temporal restriction of TH
120 signaling for PV neurons maturation, we used *Thra$^{AMI/+}$ ROSA-tdTomato$^{lox/+}$ Gad2-CreER^{T2}* mice

121 (mutants) and *Thra*$^{+/+}$ *ROSA-tdTomato*$^{lox/+}$ *Gad2-CreER*^{T2} or *Gad2-CreER*^{T2} negative mice (controls),
122 where Cre/loxP recombination can be induced at a chosen time by tamoxifen treatment.

123 A first batch of these mice were treated with tamoxifen at PND7 and histological analysis was
124 performed at PND14. This analysis revealed that expressing TRα1^{L400R} during the second postnatal
125 week was sufficient to compromise the onset of parvalbumin expression (Fig. 2a, b). But the
126 amplitude of the defect in PV expression in mutant mice was not as high as that in our previous work,
127 where TH signaling was blocked from embryonic day 12.5 to PND14 in *Thra*$^{AMI/+}$ *ROSA-tdTomato*$^{lox/+}$
128 *Gad2-Cre* mice (Richard et al., 2020). Besides, we did not observe any clear change in either the
129 density of WFA+ cells (Fig. 2a, c) or the ratio of PV+ cells that were surrounded by PNNs (Fig. 2a, d).
130 This may be due to the fact that the elaboration of PNNs mainly takes place after PND14, so that the
131 density of WFA+ cells was low, with high interindividual variability. By contrast, a tamoxifen
132 treatment performed during the fourth postnatal week (from PND21 to PND25), did not cause any
133 significant change in either PV+ cell density or WFA+ cell density at adult stage (Fig. 2e-h). Therefore,
134 THs exert their influence during a postnatal time window, which includes the second postnatal week
135 and precedes weaning, since weaning usually occurs after the end of the third postnatal week in
136 mice.

137 ***Consequences of TRα1^{L400R} expression on gene expression in neocortical GABAergic neurons two***
138 ***weeks after birth***

139 We set out to analyze the influence of TRα1^{L400R} expression on the nuclear transcriptome of
140 GABAergic neurons at PND14, a developmental stage which appears to be quite central in the
141 timeline of TH action in PV neurons. To do this, we used the *ROSA-GSL10gfp*^{lox} reporter transgene,
142 which labels cell nuclei, to extract nuclear RNA from neocortical GABAergic neurons, in which PV
143 neurons represent around 50% of the population (Tasic, Menon et al., 2016). RNA-seq analysis was
144 performed for *Thra*$^{AMI/+}$ *ROSA-GSL10gfp*$^{lox/+}$ *Gad2-Cre* mice and *Thra*$^{+/+}$ *ROSA-GSL10gfp*$^{lox/+}$ *Gad2-Cre*
145 control littermates at PND14 Differential analysis (Deseq2 adjusted p-value > 0.05; fold-change > 2.0;
146 basemean > 30) identified 275 down-regulated genes and 265 up-regulated genes in mutant mice
147 (Suppl. Table 1). This large gene set contains TRα1 target genes whose transcription is normally up-
148 regulated by liganded TRα1. Notably, among these were genes (*Hr, Klf9, Dbp, Shh, Gabrd*) that are
149 known to be TRα1 target genes in other cell types (Zekri, Guyot et al., 2022). However, many of the
150 observed changes in mRNA level probably represent indirect consequences of the long-term
151 influence of TRα1^{L400R} expression on the cell physiology.

152 To distinguish direct TRα1 target genes from other genes that are downstream in the cascade, we
153 carried out a series of additional studies. First, we looked for genes which are down-regulated by
154 hypothyroidism and up-regulated by a short TH treatment at PND14. To do this, we used a
155 propylthiouracyl (PTU) treatment to induce hypothyroidism in gestating females and their offspring.
156 Half of the hypothyroid pups with a *Thra*$^{+/+}$ *ROSA-GSL10gfp*$^{lox/+}$ *Gad2-Cre* genotype then received THs
157 at PND14. The nuclear RNA transcriptome of GABAergic neurons in the neocortex from hypothyroid
158 pups, and from pups treated with THs for 24 hours, was analyzed at PND14 as above. In this setting
159 we expected a selective recovery of mRNA level for TRα1 target genes.

160 A total of 1306 genes were sensitive to either TRα1^{L400R} expression, hypothyroidism, or TH
161 stimulation (Fig. 3a, b and Suppl. Table 1). Among them, a large set of genes were only deregulated in
162 hypothyroid mice. This suggests an important influence of hypothyroidism on the microenvironment
163 (notably glial cells) of GABAergic neurons, with indirect consequences on gene expression in
164 GABAergic neurons. The genes whose expression in GABAergic neurons was sensitive to both
165 TRα1^{L400R} expression and hypothyroidism rather reflect the cell-autonomous influence of TH signaling
166 in these neurons. Importantly, among a total of 388 of such genes was the *Pvalb* gene, which
167 encodes parvalbumin. Recovery after TH treatment (TH response reached a two-fold threshold) was
168 achieved for only a small subset of these genes (61 genes up-regulated after TH treatment and 5
169 genes down-regulated after TH treatment). However, clustering analysis revealed a clear trend
170 toward recovery, which was more visible for genes up-regulated by THs (Fig. 3c) than for genes
171 down-regulated by THs (Fig. 3d). The five genes which were down-regulated after TH treatment
172 could reflect a poorly understood negative regulation of transcription by the liganded TRα1 (Fig. 3b).
173 In the end, only 61 genes behaved as *bona fide* TRα1 target genes, with a robust negative response
174 to both TRα1^{L400R} expression and hypothyroidism, and a clear induction after the short TH treatment
175 of hypothyroid mice (Fig. 3a).

176 Gene Ontology analysis indicated that many of the genes deregulated in hypothyroid and mutant
177 mice encode components of the extracellular matrix (GO:0031012; enrichment 4.4, p-value 3.10^{-13}).
178 This includes genes encoding collagens or proteins binding to the glycosaminoglycans of PNNs
179 (GO:0005539; enrichment 4.2, p-value 5.10^{-6}). This is consistent with the hypothesis that TH/TRα1
180 signaling stimulates the elaboration of PNNs around PV neurons. The expression of two of the
181 downregulated genes in this family (*Sema7a* encoding semaphorin 7A; *Hapnl4* encoding hyaluronan
182 and proteoglycan link protein 4) was restored after a short treatment with THs, suggesting that they
183 are TRα1 target genes.

184 Another prominent characteristic of deregulated genes in hypothyroid and mutant mice was the
185 presence of genes that encode voltage-gated potassium channels (GO:0005249; enrichment 6.1, p-
186 value 10^{-6}). As these genes appeared to be sensitive to acute TH treatment, their expression is
187 unlikely to be under the direct control of TRα1. This observation suggests that hypothyroidism or
188 long-term expression of TRα1^{L400R} in GABAergic neurons damage the postnatal remodeling of ions
189 channels, which is a key event for proper maturation of PV neurons in the neocortex (Okaty et al.,
190 2009). To further evaluate this possibility, we extracted the genes that mostly encode ions channels
191 and whose expression is modified in this process of postnatal maturation, as defined by Okaty and
192 colleagues (Okaty et al., 2009). This analysis (Fig. 3e) revealed that this postnatal transition is
193 impaired and that the immature status of PV neurons persists in hypothyroid and mutant mice.

194 **Discussion**

195 In the present study, we extend our previous observations showing that a cell-autonomous action of
196 TH/TRα1 in GABAergic neurons is required for the maturation of neocortical PV neurons in mice. We
197 identified a time window that spans from birth to the end of the third postnatal week, during which
198 the action of THs is critical for the proper maturation of PV neurons. We have also found that the
199 defects induced in PV neuron maturation when TH signaling is blocked in GABAergic neurons from
200 early stages of development persist up to adulthood. Finally, analysis of gene expression at the end
201 of the second week of life pinpointed a set of genes that are directly regulated by TH/TRα1 in
202 GABAergic neurons. Some of these genes encode ion channels and PNN components, reflecting the
203 involvement of THs in essential steps of PV neuron maturation in the developing cortex.

204 Using genetically modified mouse models expressing TRα1^{L400R}, which exerts dominant negative
205 activity over TRα1, we have gathered evidence suggesting that the time window during which THs
206 promote PV neuron maturation is in the early postnatal weeks, notably during the second postnatal
207 week. First, blocking TH/TRα1 signaling in GABAergic neurons after PND7 is sufficient to alter the
208 expression of parvalbumin, as evidenced at PND14. On the contrary, blocking TH/TRα1 signaling in
209 GABAergic neurons after PND21 does not significantly alter PV neuron maturation, as assessed in
210 adulthood. PV neurons also show near-normal maturation when the blockade of TH/TRα1 signaling is
211 restricted to PV neurons and begins only after the onset of the expression of *Pvalb*, the gene that
212 encodes PV (Ren et al., 2024). Furthermore, a previous whole cortex RNA-seq analysis showed that
213 gene expression changes rapidly in wild-type mice during the second postnatal week and that this
214 evolution is stopped when TH/TRα1 signaling is blocked in GABAergic neurons (Richard et al., 2020).
215 Finally, our novel transcriptome analysis, which was carried out with sorted GABAergic neuron nuclei,
216 indicates that the postnatal maturation process of PV neurons is blunted by TRα1^{L400R} expression. In

217 particular, blocking TH/TRα1 signaling appears to compromise the expression of a number of genes
218 involved in a well-documented transition, during which the repertoire of ion channels is extensively
219 modified (Okaty et al., 2009). It is remarkable that the second postnatal week, during which THs
220 seem to play a crucial role in PV neuron maturation, coincides with a peak in circulating levels of THs
221 (Friedrichsen, Christ et al., 2003). This strongly suggests that THs represent a temporal cue to
222 synchronize the postnatal maturation of PV neurons.

223 The striking influence exerted by THs on cortical PV neuron maturation in the first postnatal weeks
224 does not exclude the possibility that THs also play a role in these neurons earlier during
225 development, or after weaning. First, we cannot fully rule out that TRα1 has an earlier function in PV
226 neurons, as recent observations suggest that it could act prenatally to promote the tangential
227 migration of GABAergic neuron progenitors (da Cunha Menezes, de Abreu et al., 2024). However,
228 there is no indication that this effect is exerted in a cell-autonomous manner. Second, a potential
229 role of THs on PV neuron maturation after weaning is supported by observations that were
230 previously reported in mice expressing TRα1^{R384C} in all tissues, for which a complete recovery in PV
231 neuron density was observed in adults (Wallis et al., 2008). By contrast, in the present study we have
232 observed little recovery in PV neuron maturation in adult mice expressing TRα1^{E395fs401} in GABAergic
233 neurons. This discrepancy is probably explained by the residual capacity of TRα1^{R384C} to bind T3 and
234 activate transcription (Tinnikov, Nordstrom et al., 2002), which is not the case for TRα1^{E395fs401}
235 (Richard et al., 2020). Therefore, the late onset of TRβ1 expression in PV neurons (Hochbaum,
236 Hulshof et al., 2024) did not appear to be sufficient to counteract the influence of the dominant
237 negative TRα1^{E395fs401} mutated receptor. Thus, up to now it is only for the first post-natal weeks that
238 there is evidence for a direct, cell-autonomous, action of THs in GABAergic neurons, impacting PV
239 neuron maturation.

240 The mode of action of THs in PV neurons during the second postnatal week is clarified by RNA-seq
241 data. In the present study, we first found that PV neurons were much more sensitive to variations in
242 TH signaling at PND14 than in adulthood, where the same method only showed minor changes in
243 gene expression (Ren et al., 2024). Another finding of the present study was that genes that were
244 consistently deregulated by blocking TH/TRα1 signaling in GABAergic neurons encode extracellular
245 matrix proteins, specific PNN components or proteins interacting with PNN glycosaminoglycans. We
246 used rapid recovery of gene expression after TH treatment in hypothyroid mice as an indication of
247 direct transcriptional control of gene expression by TRα1. This allowed us to identify a small subset of
248 genes whose deregulation is more likely to be the initial set of events preventing PV neuron
249 maturation. Among these were genes encoding transcription factors or cofactors (*Dbp, Hr, Klf9*), that

250 were already reported to be regulated by TRα1 in other contexts (Zekri et al., 2022) and that could
251 act as upstream regulators of other deregulated genes. Moreover, in this subset of putative TRα1
252 target genes, we found again genes encoding PNN components, suggesting a direct regulation of
253 PNNs by THs. Thus, it appears that liganded TRα1 might notably activate the transcription of genes
254 encoding collagens (*Col24a1* and *Col9a2* genes), ephrin A4 (*Epha4*), laminin alpha 3 subunit (*Lama3*),
255 semaphorin 7A (*Sema7a*) and hyaluronan and proteoglycan link protein 4 (*Hapln4*). This later protein
256 notably represents an essential component of the PNN (Edamatsu, Miyano et al., 2018, Nojima,
257 Miyazaki et al., 2021, Popelar, Diaz Gomez et al., 2017). Thus, a major finding of the present study is
258 that THs directly regulate the elaboration of PNNs, which is a prominent outcome of the late
259 maturation process of PV neurons.

260 The novel data presented in this paper provide strong support for the hypothesis that TH is a major
261 temporal signal for the opening and closing of the critical period of heightened plasticity, as
262 previously suggested (Batista & Hensch, 2019). The critical period occurs at slightly different times in
263 different neocortical areas, as does the onset of TH signaling (Quignodon, Legrand et al., 2004). It is
264 characterized by a series of cellular events that play a crucial role in the elaboration of functional
265 neuronal circuits (Hensch, 2005). The beginning of parvalbumin synthesis marks the opening of the
266 critical period, while the elaboration of PNNs around PV neurons stabilizes synapses and decides its
267 closure. The results presented above show that TH/TRα1 signaling directly regulate the onset of
268 parvalbumin expression, as well as the synthesis of several PNN components. Thus, our findings
269 suggest that both the opening and the closure of the critical period are directly stimulated by
270 liganded TRα1. Therefore, THs appear to act in the postnatal neocortex as it does during amphibian
271 metamorphosis, as an external cue that represents an important temporal signal. During brain
272 development, the influence of THs is also found in glial cells, as TH signaling is particularly required
273 for timely differentiation of oligodendrocytes and myelin formation (Durand & Raff, 2000, Picou,
274 Fauquier et al., 2014). Of note, oligodendrocyte maturation has also been shown to play a role in PV
275 neuron maturation and in the closure of the critical period (Kalish, Barkat et al., 2020).

276 Patients with early TH deficiency caused by congenital hypothyroidism (Van Vliet & Deladoey, 2014)
277 or carrying TRα1 mutations (van Gucht et al., 2017) are currently treated with TH replacement
278 therapy. Treatment can have a positive influence on cognitive development only if it is initiated soon
279 after birth. This is an indication that the action of THs on the maturation of the human neocortex is
280 restricted to an early temporal window, as we have found in mice. An alteration in the timing of the
281 critical period is also suspected to cause autism spectrum disorders (Sohal & Rubenstein, 2019). In
282 that regard, it is noticeable that some of the rare patients in whom *THRA* mutations have been

283 discovered were first diagnosed for autism spectrum disorders (Kalikiri, Mamidala et al., 2017, Yuen,
284 Thiruvahindrapuram et al., 2015). Within the framework of our hypothesis, the irreversible cognitive
285 and neurological defects that are seen both in patients with TH-related diseases and in patients with
286 autism spectrum disorders might be similarly regarded as consequences of a disruption of the critical
287 period of heightened cortical plasticity. We have pinpointed THs as essential players in defining the
288 critical period. Delving deeper into the detailed molecular events occurring in the neocortex during
289 the critical period will be key to finding therapeutic approaches to these debilitating pathologies.

290 *Study limitations*

291 The complete characterization of TRα1 target genes in PV neurons would require the definition of
292 chromatin occupancy by the receptor, as it informs of its presence on regulatory sequences. This is
293 not currently feasible with the small number of cells that are collected when sorting GABAergic
294 neurons from mouse neocortex. Also, the histological methods that we have used only indirectly
295 inform of the timing of the critical period of heightened plasticity, which can be defined in a number
296 of different ways (Quast, Reh et al., 2023, Reh, Dias et al., 2020).

297 **Material and methods**

298 *Mouse models and treatments*

299 Experiments involving the use of live animals for the current project were approved by local ethics
300 committees (C2EA015 and C2EA017) and subsequently authorized by the French Ministry of
301 Research (Projects #33279-2021082516194165 and #25496-2020032811174506). Mice were bred
302 and maintained at Plateau de Biologie Expérimentale de la Souris (SFR BioSciences Gerland - Lyon
303 Sud, France).

304 The *Thra*^{AMI} allele allows the expression of the dominant-negative TRα1^{L400R} after the Cre/loxP-
305 mediated deletion of a cassette with polyadenylation signals (Quignodon, Vincent et al., 2007).
306 *Thra*^{Slox} is identical, except for the presence of a C-terminus frameshift mutation which leads to the
307 expression of the dominant-negative TRα1^{E395fs401X}. The *ROSA-tdTomato*^{lox} reporter transgene (also
308 known as Ai9, MGI Cat# 4436851, RRID: MGI: 4436851) drives the Cre-dependent expression of a red
309 fluorescent protein, mainly localized in cytoplasm (Madisen, Zwingman et al., 2010). The *ROSA-*
310 *GSL10gfp*^{lox} transgene encodes the GS-EGFP-L10a protein, which is a green fluorescent protein fused
311 to the N-terminus part of the large subunit ribosomal protein L10a, mainly localized in cell nuclei
312 (Wu, Dellinger et al., 2025). All transgenes were in C57Bl6/J genetic background. *Gad2-Cre* and *Gad2-*

313 *CreER*^{T2} are knock-in alleles in which the Cre recombinase reading frame is inserted into the *Gad2*
314 gene in order to restrict the expression of the recombinase in GABAergic neurons (Taniguchi, He et
315 al., 2011). Recombination was induced in mice carrying the *Gad2-CreER*^{T2} transgene by
316 intraperitoneal injection of tamoxifen (T5648, Sigma, dissolved in sterile sunflower oil (10 mg/ml).
317 PND7 mice received a single 50 µL subcutaneous injection whereas 3-week-old mice received 5 daily
318 intraperitoneal injections (daily dose: 7.5 µL/g).

319 Gestating mice were fed for 2 weeks with iodine deficient food supplemented with 0.15% propyl-thio
320 uracyl (Envigo ref TD.95125) to cause deep hypothyroidism. TH levels were restored by a single
321 intraperitoneal injection in half of the pups (10 µg T4 + 1 µg T3 dissolved in 50 µL of phosphate buffer
322 saline, all chemicals from Sigma Aldrich France). The other PTU treated mice were injected with 50 uL
323 of phosphate buffer saline.

324 *RNA-seq analysis from sorted nuclei*

325 Nuclei were isolated from individual cortex frozen in liquid nitrogen and nuclear RNA was extracted
326 as previously described (Wu et al., 2025). Nuclear RNA was extracted from sorted nuclei (RNeasy
327 Micro Kit, Qiagen ref 74004) and quantified using Tapestation4150 (Agilent). 1 ng RNA was reverse-
328 transcribed using the SMART-Seq v4 Low Input RNA kit (Takara). cDNA was quantified and qualified
329 using Qubit (Invitrogen) and Tapestation4150 (Agilent). Libraries were then prepared from 1 ng cDNA
330 using the Nextera XT DNA Library Kit (Illumina). Libraries were sequenced (> 2.10^7 reads/library) on a
331 Nextseq500 DNA sequencer (Illumina). Reads were aligned on the mouse genome (mm10 GRCm38
332 release) with Bowtie2 (Galaxy Version 2.4.2 + galaxy 0) (Langmead, Trapnell et al., 2009). Count table
333 (Suppl. Table 1) was prepared using htseq-count (Galaxy Version 0.9.1 + galaxy 1, mode union,
334 feature type: gene) (Anders, Pyl et al., 2015). Differential gene expression analysis was performed
335 with DEseq2 (Galaxy Version 2.1.8.3) (Love, Huber et al., 2014) (Suppl. Table 1) using the following
336 thresholds: False Discovery Rate < 0.05; p-adjusted value < 0.05; maximum adjusted basecount > 30;
337 fold-change > 2.0. Hierarchical clustering was performed using Euclidian distance and complete
338 distance with Clustvis (Metsalu & Vilo, 2015). Gene Ontology analysis was performed with Gorilla
339 (https://cbl-gorilla.cs.technion.ac.il/). Raw RNA-seq data are available at NCBI Gene Expression
340 Omnibus (GSE290072 and GSE290207).

341 *Brain slice collection*

342 Each mouse was given a lethal intraperitoneal injection (6 mL/kg) of a mixture of ketamine (33
343 mg/mL) and xylazine (6.7 mg/mL). The thorax was opened and each mouse was perfused with 3.7%

344 paraformaldehyde in 0.1 M phosphate buffer at room temperature. Each brain was dissected out,
345 immersed in fixative at 4°C for 3 h and then in phosphate buffered saline (PBS) at 4°C until sectioning.
346 Coronal sections (50 µm) were cut with the aid of a vibrating microtome (Integraslice 7550 SPDS,
347 Campden Instruments, Loughborough, UK), in PBS at room temperature. Brain sections were stored
348 at -20°C in cryoprotectant (30% ethylene glycol and 20% glycerol in 10 mM low-salt PBS).

349 *Brain slice histology*

350 Immunohistochemistry was performed on free-floating brain sections. For PV labeling, a mouse anti-
351 PV primary antibody (PARV19, Sigma P3088, 1:2000), and a secondary antibody made in donkey
352 (anti-mouse DyLight 633, ThermoFisher Scientific, 1:1000) were used. For the concurrent PNN
353 labeling, a biotinylated Wisteria floribunda lectin (WFL/WFA, Vector Laboratories B-1355, 20 µg/mL),
354 and Streptavidin coupled to DyLight 488 (Vector Laboratories, SA-5488, 1:1000) were used. Non-
355 specific binding sites were blocked by incubating sections for 1 h in PBS with 1% BSA and 0.2% Triton
356 X100. Brain sections were incubated overnight at 4°C with PV antibody and biotinylated WFA, which
357 were diluted in PBS with 1% BSA, 0.2% Triton X-100 and 1% dimethyl sulfoxide. Sections were
358 washed in PBS and further incubated for 15 min at room temperature with DAPI (4',6-diamidino-2-
359 phenylindole, 1:5000, Sigma). Incubation with the secondary antibody lasted for 3 h at room
360 temperature. Sections were mounted in Fluoroshield™ (Sigma), coverslipped and imaged using an
361 inverted confocal microscope (Zeiss LSM 780 and Zeiss LSM 800).

362 *Image analysis*

363 Image analysis was performed using ImageJ. Final images resulted from the z projection of 3 optical
364 sections (Maximum intensity tool) that were 2 µm apart (the resulting images thus reflected the
365 fluorescence collected over a thickness of 4 µm). PV+ WFA+ Tomato+ cells were detected from final
366 images using the Cellpose wrapper for Fiji (Stringer, Wang et al., 2021). Numbers of mono-, double-
367 or triple-labelled cells per slice were measured automatically from 3-4 slices per mouse. The code of
368 the original macro may be found here: https://github.com/jbrocardplatim/MacroPV

369 The densities of Tomato+, PV+, WFA+ cells, and their co-localizations were counted in the whole area
370 of one image taken in the somatosensory cortex area. 3-4 images in each hemisphere were analyzed
371 for each mouse. Quantitative data were analyzed using two-tailed unpaired T-test. Data are
372 expressed as mean ± SEM. Data analyses were performed with Excel 2016 and GraphPad Prism
373 software (v.8.). The level of significance was set at $p < 0.05$.

374

375 **References**

376 Anders S, Pyl PT, Huber W (2015) HTSeq--a Python framework to work with high-throughput
377 sequencing data. *Bioinformatics* 31: 166-9
378 Batista G, Hensch TK (2019) Critical Period Regulation by Thyroid Hormones: Potential Mechanisms
379 and Sex-Specific Aspects. *Front Mol Neurosci* 12: 77
380 Berbel P, Navarro D, Roman GC (2014) An evo-devo approach to thyroid hormones in cerebral and
381 cerebellar cortical development: etiological implications for autism. *Front Endocrinol (Lausanne)* 5:
382 146
383 Bernal J, Morte B, Diez D (2022) Thyroid hormone regulators in human cerebral cortex development.
384 *J Endocrinol* 255: R27-R36
385 da Cunha Menezes E, de Abreu FF, Davis JB, Maurer SV, Roshko VC, Richardson A, Dowell J, Cassella
386 SN, Stevens HE (2024) Effects of gestational hypothyroidism on mouse brain development: Gabaergic
387 systems and oxidative stress. *Dev Biol* 515: 112-120
388 de Lecea L, del Rio JA, Soriano E (1995) Developmental expression of parvalbumin mRNA in the
389 cerebral cortex and hippocampus of the rat. *Brain Res Mol Brain Res* 32: 1-13
390 del Rio JA, de Lecea L, Ferrer I, Soriano E (1994) The development of parvalbumin-immunoreactivity
391 in the neocortex of the mouse. *Brain Res Dev Brain Res* 81: 247-59
392 Durand B, Raff M (2000) A cell-intrinsic timer that operates during oligodendrocyte development.
393 *Bioessays* 22: 64-71
394 Edamatsu M, Miyano R, Fujikawa A, Fujii F, Hori T, Sakaba T, Oohashi T (2018) Hapln4/Bral2 is a
395 selective regulator for formation and transmission of GABAergic synapses between Purkinje and
396 deep cerebellar nuclei neurons. *J Neurochem* 147: 748-763
397 Friedrichsen S, Christ S, Heuer H, Schafer MK, Mansouri A, Bauer K, Visser TJ (2003) Regulation of
398 iodothyronine deiodinases in the Pax8-/- mouse model of congenital hypothyroidism. *Endocrinology*
399 144: 777-84
400 Gilbert ME, Sui L, Walker MJ, Anderson W, Thomas S, Smoller SN, Schon JP, Phani S, Goodman JH
401 (2007) Thyroid hormone insufficiency during brain development reduces parvalbumin
402 immunoreactivity and inhibitory function in the hippocampus. *Endocrinology* 148: 92-102
403 Hensch TK (2005) Critical period plasticity in local cortical circuits. *Nat Rev Neurosci* 6: 877-88
404 Hijazi S, Smit AB, van Kesteren RE (2023) Fast-spiking parvalbumin-positive interneurons in brain
405 physiology and Alzheimer's disease. *Mol Psychiatry* 28: 4954-4967

406 Hochbaum DR, Hulshof L, Urke A, Wang W, Dubinsky AC, Farnsworth HC, Hakim R, Lin S, Kleinberg G,
407 Robertson K, Park C, Solberg A, Yang Y, Baynard C, Nadaf NM, Beron CC, Girasole AE, Chantranupong
408 L, Cortopassi MD, Prouty S et al. (2024) Thyroid hormone remodels cortex to coordinate body-wide
409 metabolism and exploration. *Cell* 187: 5679-5697 e23
410 Huang ZJ, Kirkwood A, Pizzorusso T, Porciatti V, Morales B, Bear MF, Maffei L, Tonegawa S (1999)
411 BDNF regulates the maturation of inhibition and the critical period of plasticity in mouse visual
412 cortex. *Cell* 98: 739-55
413 Kalikiri MK, Mamidala MP, Rao AN, Rajesh V (2017) Analysis and functional characterization of
414 sequence variations in ligand binding domain of thyroid hormone receptors in autism spectrum
415 disorder (ASD) patients. *Autism research : official journal of the International Society for Autism*
416 *Research*
417 Kalish BT, Barkat TR, Diel EE, Zhang EJ, Greenberg ME, Hensch TK (2020) Single-nucleus RNA
418 sequencing of mouse auditory cortex reveals critical period triggers and brakes. *Proc Natl Acad Sci U*
419 *S A* 117: 11744-11752
420 Langmead B, Trapnell C, Pop M, Salzberg SL (2009) Ultrafast and memory-efficient alignment of short
421 DNA sequences to the human genome. *Genome biology* 10: R25
422 Love MI, Huber W, Anders S (2014) Moderated estimation of fold change and dispersion for RNA-seq
423 data with DESeq2. *Genome biology* 15: 550
424 Madisen L, Zwingman TA, Sunkin SM, Oh SW, Zariwala HA, Gu H, Ng LL, Palmiter RD, Hawrylycz MJ,
425 Jones AR, Lein ES, Zeng H (2010) A robust and high-throughput Cre reporting and characterization
426 system for the whole mouse brain. *Nature neuroscience* 13: 133-40
427 Markossian S, Guyot R, Richard S, Teixeira M, Aguilera N, Bouchet M, Plateroti M, Guan W, Gauthier
428 K, Aubert D, Flamant F (2018) CRISPR/Cas9 Editing of the Mouse Thra Gene Produces Models with
429 Variable Resistance to Thyroid Hormone. *Thyroid* 28: 139-150
430 Mayerl S, Heuer H (2023) Thyroid hormone transporter Mct8/Oatp1c1 deficiency compromises
431 proper oligodendrocyte maturation in the mouse CNS. *Neurobiol Dis* 184: 106195
432 Metsalu T, Vilo J (2015) ClustVis: a web tool for visualizing clustering of multivariate data using
433 Principal Component Analysis and heatmap. *Nucleic Acids Res* 43: W566-70
434 Nojima K, Miyazaki H, Hori T, Vargova L, Oohashi T (2021) Assessment of Possible Contributions of
435 Hyaluronan and Proteoglycan Binding Link Protein 4 to Differential Perineuronal Net Formation at
436 the Calyx of Held. *Front Cell Dev Biol* 9: 730550
437 Okaty BW, Miller MN, Sugino K, Hempel CM, Nelson SB (2009) Transcriptional and
438 electrophysiological maturation of neocortical fast-spiking GABAergic interneurons. *The Journal of*
439 *neuroscience : the official journal of the Society for Neuroscience* 29: 7040-52

440 Picou F, Fauquier T, Chatonnet F, Richard S, Flamant F (2014) Deciphering direct and indirect
441 influence of thyroid hormone with mouse genetics. *Mol Endocrinol* 28: 429-41
442 Popelar J, Diaz Gomez M, Lindovsky J, Rybalko N, Burianova J, Oohashi T, Syka J (2017) The absence
443 of brain-specific link protein Bral2 in perineuronal nets hampers auditory temporal resolution and
444 neural adaptation in mice. *Physiol Res* 66: 867-880
445 Quast KB, Reh RK, Caiati MD, Kopell N, McCarthy MM, Hensch TK (2023) Rapid synaptic and gamma
446 rhythm signature of mouse critical period plasticity. *Proc Natl Acad Sci U S A* 120: e2123182120
447 Quignodon L, Legrand C, Allioli N, Guadano-Ferraz A, Bernal J, Samarut J, Flamant F (2004) Thyroid
448 hormone signaling is highly heterogeneous during pre- and postnatal brain development. *J Mol*
449 *Endocrinol* 33: 467-76
450 Quignodon L, Vincent S, Winter H, Samarut J, Flamant F (2007) A point mutation in the activation
451 function 2 domain of thyroid hormone receptor alpha1 expressed after CRE-mediated recombination
452 partially recapitulates hypothyroidism. *Mol Endocrinol* 21: 2350-60
453 Reh RK, Dias BG, Nelson CA, 3rd, Kaufer D, Werker JF, Kolb B, Levine JD, Hensch TK (2020) Critical
454 period regulation across multiple timescales. *Proc Natl Acad Sci U S A* 117: 23242-23251
455 Ren J, Flamant F (2023) Thyroid hormone as a temporal switch in mouse development. *Eur Thyroid J*
456 12
457 Ren J, Markossian S, Guyot R, Aubert D, Li D, Cauli B, Riet F, Wong J, Flamant F, Richard S (2024)
458 Thyroid hormones maintain parvalbumin neuron functions in mouse neocortex. *bioRxiv*:
459 2024.07.16.603713
460 Richard S, Guyot R, Rey-Millet M, Prieux M, Markossian S, Aubert D, Flamant F (2020) A Pivotal
461 Genetic Program Controlled by Thyroid Hormone during the Maturation of GABAergic Neurons.
462 *iScience* 23: 100899
463 Richard S, Ren J, Flamant F (2023) Thyroid hormone action during GABAergic neuron maturation: The
464 quest for mechanisms. *Front Endocrinol (Lausanne)* 14: 1256877
465 Sohal VS, Rubenstein JLR (2019) Excitation-inhibition balance as a framework for investigating
466 mechanisms in neuropsychiatric disorders. *Mol Psychiatry* 24: 1248-1257
467 Stringer C, Wang T, Michaelos M, Pachitariu M (2021) Cellpose: a generalist algorithm for cellular
468 segmentation. *Nat Methods* 18: 100-106
469 Takesian AE, Hensch TK (2013) Balancing plasticity/stability across brain development. *Prog Brain Res*
470 207: 3-34
471 Taniguchi H, He M, Wu P, Kim S, Paik R, Sugino K, Kvitsiani D, Fu Y, Lu J, Lin Y, Miyoshi G, Shima Y,
472 Fishell G, Nelson SB, Huang ZJ (2011) A resource of Cre driver lines for genetic targeting of GABAergic
473 neurons in cerebral cortex. *Neuron* 71: 995-1013

474 Tasic B, Menon V, Nguyen TN, Kim TK, Jarsky T, Yao Z, Levi B, Gray LT, Sorensen SA, Dolbeare T,
475 Bertagnolli D, Goldy J, Shapovalova N, Parry S, Lee C, Smith K, Bernard A, Madisen L, Sunkin SM,
476 Hawrylycz M et al. (2016) Adult mouse cortical cell taxonomy revealed by single cell transcriptomics.
477 *Nature neuroscience* 19: 335-46
478 Tinnikov A, Nordstrom K, Thoren P, Kindblom JM, Malin S, Rozell B, Adams M, Rajanayagam O,
479 Pettersson S, Ohlsson C, Chatterjee K, Vennstrom B (2002) Retardation of post-natal development
480 caused by a negatively acting thyroid hormone receptor alpha1. *Embo J* 21: 5079-87
481 Uchida K, Hasuoka K, Fuse T, Kobayashi K, Moriya T, Suzuki M, Katayama N, Itoi K (2021) Thyroid
482 hormone insufficiency alters the expression of psychiatric disorder-related molecules in the
483 hypothyroid mouse brain during the early postnatal period. *Sci Rep* 11: 6723
484 van Gucht ALM, Moran C, Meima ME, Visser WE, Chatterjee K, Visser TJ, Peeters RP (2017)
485 Resistance to Thyroid Hormone due to Heterozygous Mutations in Thyroid Hormone Receptor Alpha.
486 *Current topics in developmental biology* 125: 337-355
487 Van Vliet G, Deladoey J (2014) Diagnosis, treatment and outcome of congenital hypothyroidism.
488 *Endocr Dev* 26: 50-9
489 Wallis K, Sjogren M, van Hogerlinden M, Silberberg G, Fisahn A, Nordstrom K, Larsson L, Westerblad
490 H, Morreale de Escobar G, Shupliakov O, Vennstrom B (2008) Locomotor deficiencies and aberrant
491 development of subtype-specific GABAergic interneurons caused by an unliganded thyroid hormone
492 receptor alpha1. *The Journal of neuroscience : the official journal of the Society for Neuroscience* 28:
493 1904-15
494 Wingert JC, Sorg BA (2021) Impact of Perineuronal Nets on Electrophysiology of Parvalbumin
495 Interneurons, Principal Neurons, and Brain Oscillations: A Review. *Front Synaptic Neurosci* 13:
496 673210
497 Wu S, Dellinger J, Markossian S, Dusabyinema Y, Guyot R, Hughes S, Aubert D, Fackeure M, Gauthier
498 K, Gillet B, Jiang W, Flamant F (2025) An Atlas of Thyroid Hormone Responsive Genes in Adult Mouse
499 Hypothalamus. *Endocrinology* 166
500 Yuen RK, Thiruvahindrapuram B, Merico D, Walker S, Tammimies K, Hoang N, Chrysler C,
501 Nalpathamkalam T, Pellecchia G, Liu Y, Gazzellone MJ, D'Abate L, Deneault E, Howe JL, Liu RS,
502 Thompson A, Zarrei M, Uddin M, Marshall CR, Ring RH et al. (2015) Whole-genome sequencing of
503 quartet families with autism spectrum disorder. *Nature medicine* 21: 185-91
504 Zekri Y, Guyot R, Flamant F (2022) An Atlas of Thyroid Hormone Receptors' Target Genes in Mouse
505 Tissues. *Int J Mol Sci* 23

506 **Figure legends:**

507 **Fig. 1 | Persistent defect in PV neuron maturation in mice expressing TRα1^{E395fs401X}.** Histological
508 analysis of *Thra*$^{+/+}$ *ROSA-tdTomato*$^{lox/+}$ *Gad2-Cre* littermates (controls) and *Thra*$^{Slox/+}$ *ROSA-*
509 *tdTomato*$^{lox/+}$ *Gad2-Cre* mice (mutants) that express TRα1^{E395fs401X} in the GABAergic neurons and their
510 progenitors from embryonic day 12.5 to PND21 (**a-d**, controls: n = 6, mutants: n = 6) and to adult
511 stage (**e-h**, controls: n = 6, mutants: n = 5). **a, e** Immunohistochemistry of parvalbumin and WFA-
512 labeled PNNs in PV neurons of somatosensory cortex at striatum level. **b, f** The density of PV+ cells
513 was lower in mutants at both ages. **c, g** The density of WFA+ cells was lower in mutants at both ages.
514 **d, h** The proportion of PV neurons surrounded by PNNs was lower in mutants at both ages. Data are
515 presented as mean ± SEM and analyzed using an unpaired two-tailed T-test (*$p < 0.05$, **$p < 0.01$,
516 ***$p < 0.001$). Also see Suppl. Fig. 1 for related analyses.

517 **Fig. 2 | A time window for TH action on PV neuron maturation.** Histological analysis of *Thra*$^{+/+}$ *ROSA-*
518 *tdTomato*$^{lox/+}$ *Gad2-CreER*^{T2} or *Gad2-CreER*^{T2} negative littermates (controls) and *Thra*$^{AMI/+}$ *ROSA-*
519 *tdTomato*$^{lox/+}$ *Gad2-CreER*^{T2} mice (mutants) that express TRα1^{L400R} in the GABAergic lineage from
520 PND7 to PND14 (**a-d**, controls: n = 8, mutants: n = 6) and from PND21 to adult (**e-h**, controls: n = 11,
521 mutants: n = 7). **a, e** Immunohistochemistry of parvalbumin and WFA-labeled PNNs in PV neurons of
522 somatosensory cortex at striatum level. **b, f** The density of PV+ cells was lower in mutants in former
523 but not in latter. **c, g** The density of WFA+ cells had no clear difference in both cases. **d, h** The
524 proportion of PV neurons surrounded by PNNs had no clear difference in both cases. Data are
525 presented as mean ± SEM and analyzed using unpaired two-tailed T-test (*$p < 0.05$, **$p < 0.01$, ***p
526 < 0.001).

527 **Fig. 3 | RNA-seq analysis of gene expression in sorted GABAergic neuron nuclei.** Nuclei were sorted
528 at PND14 from the neocortex of *Thra*$^{+/+}$ *ROSA-GSL10gfp*^{lox} *Gad2-Cre* mice (Ctrl), *Thra*$^{AMI/+}$ *ROSA-*
529 *GSL10gfp*^{lox} *Gad2-Cre* mice expressing TRα1^{L400R} in GABAergic neurons (Mut), hypothyroid *Thra*$^{+/+}$
530 *ROSA-GSL10gfp*^{lox} *Gad2-Cre* mice (Hypoth.), or hypothyroid *Thra*$^{+/+}$ *ROSA-GSL10gfp*^{lox} *Gad2-Cre* mice
531 that received a single TH injection at PND13 (+TH). **a** Venn diagram of genes that were either
532 downregulated by TRα1^{L400R}, downregulated by hypothyroidism or induced after TH treatment. **b**
533 Venn diagram of genes that were either upregulated by TRα1^{L400R}, upregulated by hypothyroidism or
534 repressed after TH treatment (thresholds: Fold change > 2 or < 0.5, maximal adjusted base counts >
535 30, adjusted p-value > 0.05). **c** Heatmap showing the genes that were downregulated by both
536 TRα1^{L400R} and hypothyroidism. Note the variable response to TH. **d** Heatmap showing the genes that
537 were upregulated by both TRα1^{L400R} and hypothyroidism. **e** Heatmap of markers of PV neuron
538 maturation. The marks on the right side are for genes whose expression normally increases (red) or
539 decreases (green) between PND7 and PND21. The alterations of gene expression in mutant mice

540 reveals a blockade of the PV neuron maturation program, caused either by TRα1^{L400R} expression or by
541 hypothyroidism. A 24h TH treatment two weeks after birth is not sufficient to restore the expression
542 of these marker genes. Also see Suppl. Table 1 for related datasets.

543

544

Acknowledgements:

We acknowledge the contribution of SFR Biosciences (Université Claude Bernard Lyon 1, CNRS UAR3444, Inserm US8, ENS de Lyon): Nadine Aguilera and the Plateau de Biologie Expérimentale de la Souris (ANIRA-PBES) for mouse breeding; ANIRA-CYTOMETRIE and particularly Sébastien Dussurgey for nuclei sorting; ANIRA-AGC for mouse genotyping. We thank Benjamin Gillet and Sandrine Hughes of the deep sequencing facility (PSI IGFL, Lyon). We also thank Elodie Martel for carrying out histology experiments as part of her internships and Isabelle Dusart (Institut de Biologie Paris Seine, France) for helpful discussions. We acknowledge China Scholarship Council for a scholarship to Juan REN to do her PhD project in ENS de Lyon. Research fundings were from European Union's Horizon 2020 research and innovation program, under grant agreement No. 825753 (ERGO), Agence Nationale de la Recherche (Thyromut2 program; ANR-15-CE14-0011-01).

Disclosure and competing interests statement

The authors have nothing to declare.

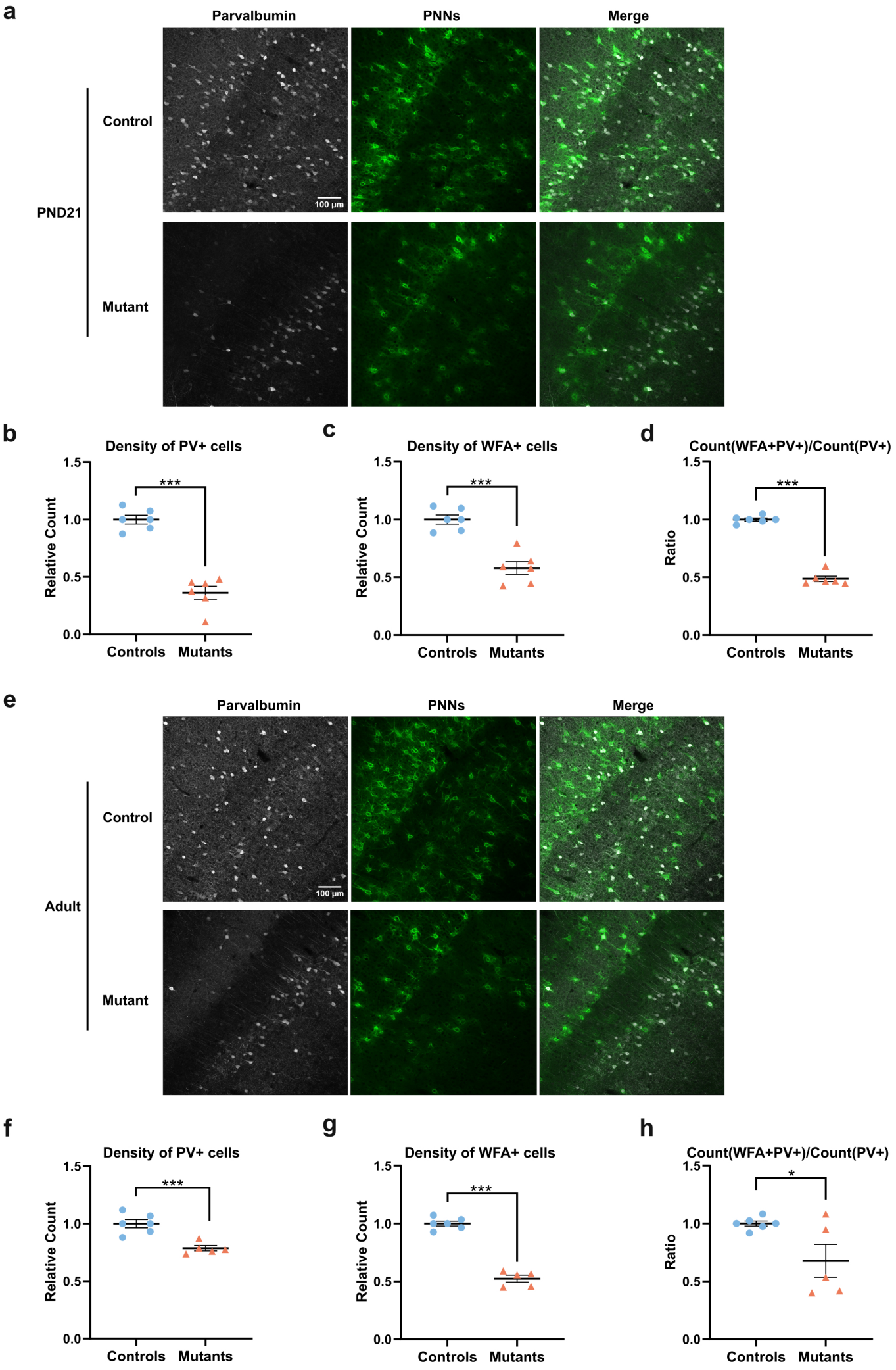
a
Parvalbumin
PNNs
Merge
PND21
Control
Mutant
100 µm
b
Density of PV+ cells
Relative Count
1.5
1.0
0.5
0.0
***
Controls
Mutants
c
Density of WFA+ cells
Relative Count
1.5
1.0
0.5
0.0
***
Controls
Mutants
d
Count(WFA+PV+)/Count(PV+)
Ratio
1.5
1.0
0.5
0.0
***
Controls
Mutants
e
Parvalbumin
PNNs
Merge
Adult
Control
Mutant
100 µm
f
Density of PV+ cells
Relative Count
1.5
1.0
0.5
0.0
***
Controls
Mutants
g
Density of WFA+ cells
Relative Count
1.5
1.0
0.5
0.0
***
Controls
Mutants
h
Count(WFA+PV+)/Count(PV+)
Ratio
1.5
1.0
0.5
0.0
*
Controls
Mutants

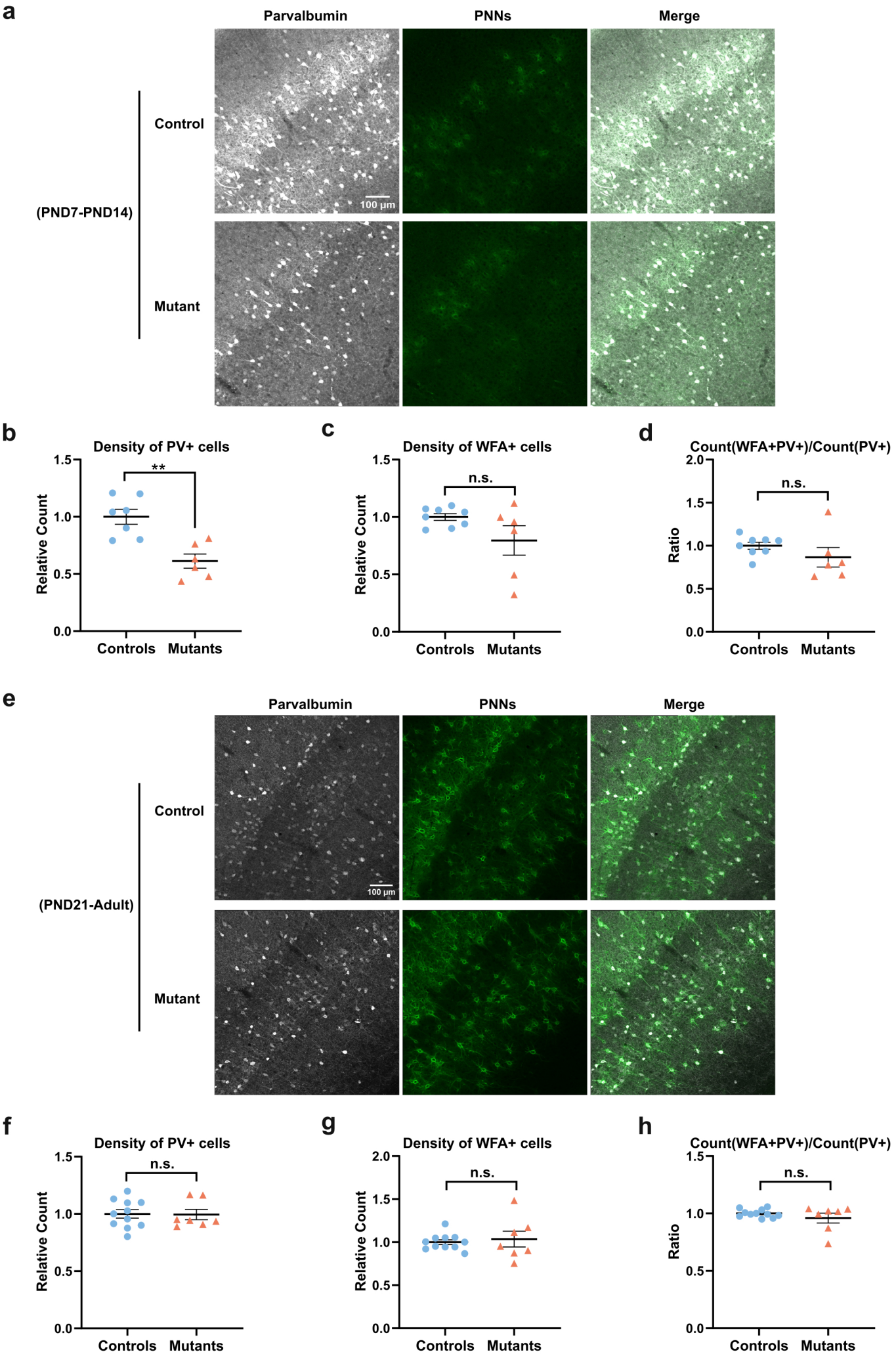
a
Parvalbumin
PNNs
Merge
Control
(PND7-PND14)
Mutant
100 µm
b
Density of PV+ cells
Relative Count
**
Controls
Mutants
c
Density of WFA+ cells
Relative Count
n.s.
Controls
Mutants
d
Count(WFA+PV+)/Count(PV+)
Ratio
n.s.
Controls
Mutants
e
Parvalbumin
PNNs
Merge
Control
(PND21-Adult)
Mutant
100 µm
f
Density of PV+ cells
Relative Count
n.s.
Controls
Mutants
g
Density of WFA+ cells
Relative Count
n.s.
Controls
Mutants
h
Count(WFA+PV+)/Count(PV+)
Ratio
n.s.
Controls
Mutants

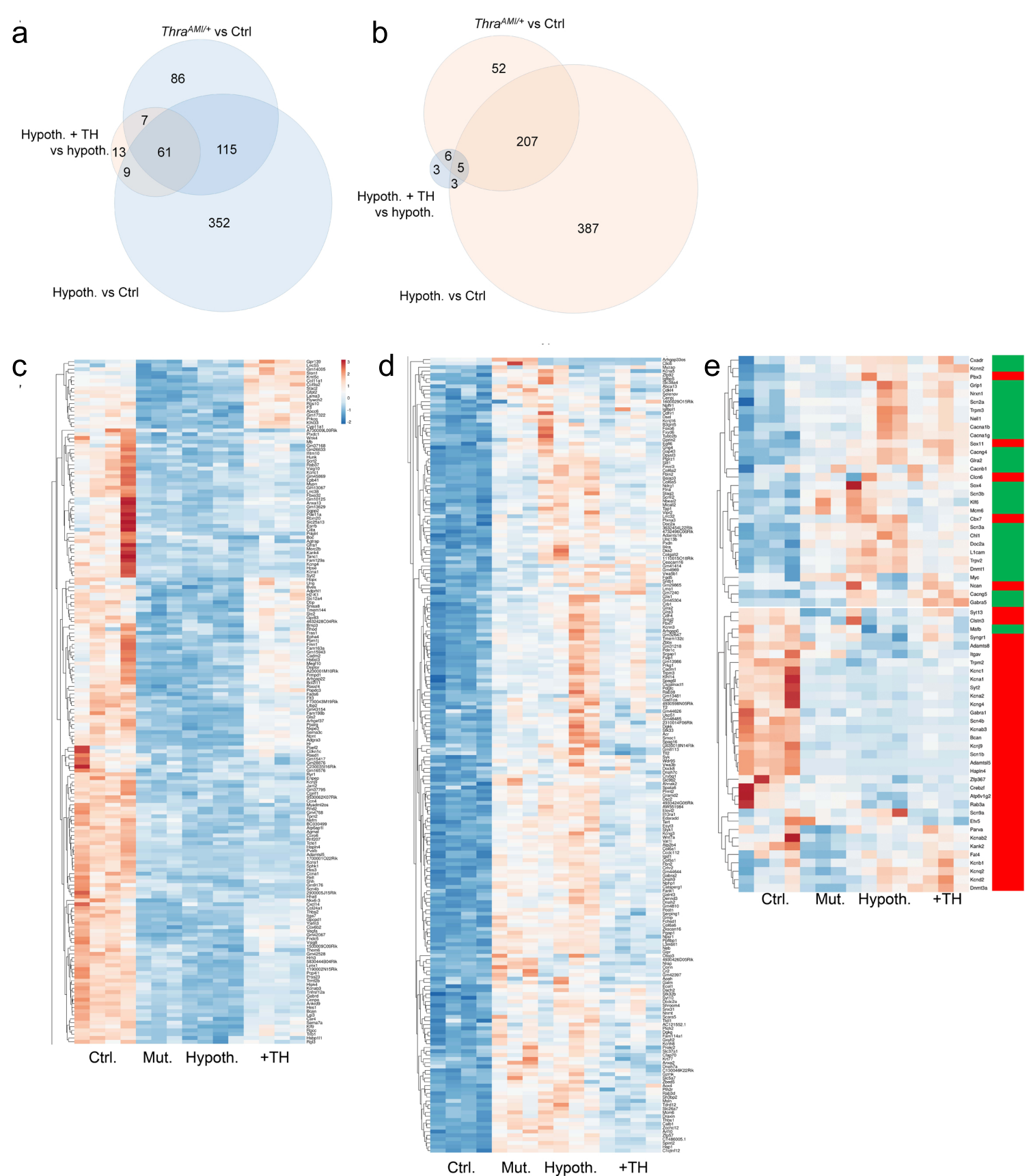
a
Thra^AMI/+ vs Ctrl
86
7
Hypoth. + TH
vs hypoth.
13
61
115
9
352
Hypoth. vs Ctrl
b
Thra^AMI/+ vs Ctrl
52
207
6
3
5
3
Hypoth. + TH
vs hypoth.
387
Hypoth. vs Ctrl
c
Ctrl.
Mut.
Hypoth.
+TH
d
Ctrl.
Mut.
Hypoth.
+TH
e
Ctrl.
Mut.
Hypoth.
+TH